
OCTAL: Graph Representation Learning for LTL Model Checking

Prasita Mukherjee, Haoteng Yin, Susheel Suresh, Tiark Rompf

Department of Computer Science, Purdue University
{mukher39,yinht,suresh43,tiark}@purdue.edu

Abstract

Model Checking is widely applied in verifying the correctness of complex and concurrent systems against a specification. Pure symbolic approaches while popular, still suffer from the state space explosion problem that makes them impractical for large scale systems and/or specifications. In this paper, we propose to use graph representation learning (GRL) for solving linear temporal logic (LTL) model checking, where the system and the specification are expressed by a Büchi automaton and an LTL formula respectively. A novel GRL-based framework OCTAL, is designed to learn the representation of the graph-structured system and specification, which reduces the model checking problem to binary classification in the latent space. The empirical experiments show that OCTAL achieves comparable accuracy against canonical SOTA model checkers on three different datasets, with up to $5\times$ overall speedup and above $63\times$ for satisfiability checking alone.

1 Introduction

Model checking, proposed by Clarke et al. [12] is defined as the problem of deciding whether a specification holds for all executions of a system, where a property is typically specified in a temporal logic like Linear Temporal Logic (LTL), Computational Tree Logic (CTL), etc. Model checking has proven to be extremely effective in verifying complex systems against a set of specifications. It has gained wide acceptance in the fields of systems engineering [4], protocol verification in hardware and software systems [31], malware detection and security protocols [2].

Generally, formal specifications are expressed using temporal logic formulae like LTL, CTL, etc. The system/model is expressed using automata like Büchi [10], Muller, Kripke structures [36], or, Petri nets [34] to express concurrent systems. Given the system and the specification expressed using temporal logic, model checking can automatically verify whether the system satisfies the specification. The result of model checking on a system expressed in Büchi automaton will be ‘1/true’ if the automaton satisfies the given specification expressed in temporal logic, and ‘0/false’ otherwise.

Linear Temporal Logic (LTL) [35] and Computational Tree Logic (CTL) [18, 6] are the two most widely used temporal logics to express a specification both in industry and academia. Traditionally, LTL model checking first computes the automaton B_{\neg} corresponding to the negation of the given LTL formula, followed by cross product of the system B with the negation B_{\neg} , and then checks for the emptiness of the product (illustrated in Figure 1). However, this approach suffers from the state space explosion problem [39] which severely hinders the performance of a model checker, especially when LTL formulae map to exponentially sized systems and the subsequent graph product computation. Methods such as partial order reduction [22], symmetry [14, 13], bounded model checking [7, 23], and equivalence relations have been proposed to address this problem. Some progress has been made by these methods, but the problem of exploded state space remains hard in general. Hence, it still constitutes a major bottleneck in many applications of model checking.

Recently, machine learning (ML) techniques [5, 43] have gained great success in dealing with the state space explosion problem. Zhu et al. [43] used machine learning algorithms like random forest, decision trees to predict whether a system (Kripke structure) satisfies a specification (LTL formula). Behjati et al. [5] proposed a reinforcement learning based approach for on-the-fly model checking of properties expressed with LTL formulae. Although not guaranteed to be 100% accurate, leaning-based approaches are much *faster* and *cheaper* compared to traditional model checkers (MCs) as they avoid computing the cross product of the system and specification. Furthermore, it is especially useful in scenarios where traditional MCs time out/fail to solve, while *speed* and *efficiency* are the key factors. For instance, in software verification, traditional MCs are not always a viable choice due to their high cost. Consider a large software development effort, where it would be favorable to use a MC to ascertain a higher degree of correctness than pure testing. In such large-scale deployments, classical MCs often take prohibitively long time for verification, especially when the system under test has an exponential state space. In this case, only ML-based MCs can provide a practical solution, which broadens the applicability of MCs by trading off some amount of accuracy guarantees for better running time and scalability, and is particularly promising for large systems and/or specifications.

However, previous work of ML-based MCs either does not generalize well across systems and specifications with varying lengths [43], or cater to bounded model checking [5]. Such limitations can be well addressed through more powerful and expressive frameworks, e.g. representation learning. Due to the structural essence of the input, model checking can be naturally formulated into graph tasks. This motivates us to propose a novel graph representation learning (GRL) based framework, OCTAL, to tackle this challenging problem and perform LTL model checking. For a given input, the system is expressed as a Büchi automaton B and the specification with an LTL formula ϕ . Then, OCTAL determines whether B satisfies ϕ by reducing the problem to binary classification on graph-structured data representing the given system and the specification. Here, the Büchi automaton is encoded as a bipartite graph and the LTL formula is presented as an expression tree. Instead of modeling them separately, we employ the union operation to obtain their unified graph structures and learn the *joint graph representation* for classification with the output ‘0/1’. LTL’s expression tree representation and graph union operations avoid the construction of system corresponding to the specification, followed by the cross product. When it comes to polynomial sized systems and LTL formulae that map to exponentially sized systems, through this formulation, we can reduce the model checking problem to graph classification that prevents us from encountering the state space explosion problem.

We performed extensive experiments on OCTAL, traditional MCs and neural network baselines for LTL model checking, in terms of both accuracy and speed on three datasets: one from open competition RERS19 [27] and two new ones specifically constructed for this task. Experimental results show that OCTAL consistently achieves $\sim 90\%$ precision and recall on all three datasets, which indicates its great generalization ability on unseen data and its high utility in practice. Meanwhile, the performance of OCTAL is not negatively affected by the varying length of LTL formulae and systems present in our specially designed dataset *Diverse* as other ML-based MCs in [43] would be. In general, OCTAL is up to $5\times$ faster than the state-of-the-art traditional MCs with over 90% accuracy, and achieves over $63\times$ speedup in term of inference alone. Our major contribution can be summarized as follows: 1) LTL model checking is firstly formulated as a representation learning task, where the system and the specification are expressed in graph-structured data. 2) A new paradigm of model checking is proposed. To represent and bridge structural/semantic correspondence between LTL and Büchi automaton, the cross product is replaced by computationally cheaper graph union operations. 3) Two new datasets are constructed for LTL model checking benchmark: *Short* with large amount of short-size LTL samples and *Diverse* with more complex and varied-length samples.

2 Preliminaries

2.1 Büchi Automata

In automata theory, a Büchi automaton (BA) is a system that either accepts or rejects inputs of infinite length. The automaton is represented by a set of states (one initial, some final, and others neither initial nor final), a transition relation, which determines which state should the present state move to, depending on the alphabets that hold in the transition. The system accepts an input if and only if it visits at least one accepting state infinitely often for the input. A Büchi automaton can be

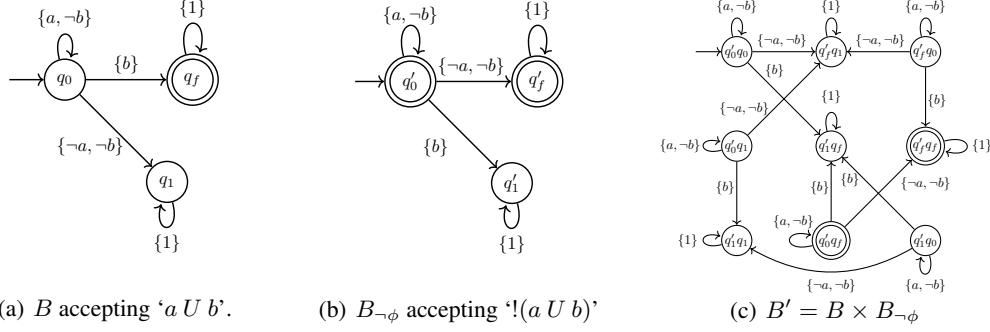


Figure 1: Illustration of systems B , $B_{\neg\phi}$ and their product B' . B accepts ' $a U b$ ', meaning a must be true until b becomes true. $B_{\neg\phi}$ accepts ' $!(a U b)$ ', where $\neg\phi$ is the negation of ' $a U b$ '. B' is the cross product of B and $B_{\neg\phi}$, which significantly increases the state size.

deterministic or non-deterministic. We deal with non-deterministic Büchi automata systems in this paper, as they are strictly more powerful than deterministic Büchi automata systems.

A non-deterministic Büchi automaton B is formally defined as the tuple $(Q, \Sigma, \Delta, q_0, \mathbf{q}_f)$, where Q is the set of all states of B , and is finite; Σ is the finite set of alphabets; $\Delta : Q \times 2^\Sigma \rightarrow 2^Q$ is the transition relation that can map a state to a set of states on the same input set; $q_0 \in Q$ represents the initial state; $\mathbf{q}_f \subset Q$ is the set of final states.

2.2 Linear Temporal Logic

Linear Temporal Logic (LTL), is a type of temporal logic that models properties with respect to time. An LTL formula is constructed from a finite set of atomic propositions, logical operators not (!), and (&), and or (|), true (1), false (N), and temporal operators. Additional logical operators such as implies, equivalence, etc. that can be replaced by the combination of basic logical operators (!, &, |). For example, $a \rightarrow b$ is expressed as $!a | b$.

2.3 LTL Model Checking

Given a Büchi automaton B (system), and an LTL formula ϕ (specification), the model checking problem decides whether B satisfies ϕ . Traditionally, the problem is solved by computing the Büchi automaton for the negation of the specification ϕ as $B_{\neg\phi}$, followed by the product automaton $B' = B \times B_{\neg\phi}$. The problem then reduces to checking the language emptiness of B' . The language accepted by B' is said to be empty if and only if B' rejects all inputs. Construction of B is linear in the size of its state space, while $B_{\neg\phi}$ is exponential in the size of $\neg\phi$. The product construction would also lead to an automaton of size $|B| \times 2^{|\neg\phi|}$, which can blow up even ϕ is linear in the size of B , leading to the state space explosion problem. Figure 1(a) represents the system B with ϕ : ' $a U b$ ', and Figure 1(b) represents $B_{\neg\phi}$. The cross product $B' = B \times B_{\neg\phi}$ is given in Figure 1(c). B' does not accept anything as there is no feasible path from the initial state (q_0q_0) to either of the final states ($q'_0q_f, q'_f q_f$). Here, both B and $B_{\neg\phi}$ are three times smaller than B' in terms of the number of states, and 6 times smaller regarding the number of transitions. As observed in Figure 1, it can be concluded that even for moderately complex specifications, the product can still result in an exponential state space, which would severely hinder the performance of traditional model checkers.

2.4 Graph Neural Networks

Graph Neural Networks (GNN) extend regular neural networks to better support representation learning in graph domains. A GNN takes the input formed as a graph $\mathcal{G} = (\mathcal{V}, \mathcal{E})$, where $\mathcal{V} = [n]$ represents the node set and $\mathcal{E} \subseteq \mathcal{V} \times \mathcal{V}$ is the edge set. The graph can be directed or undirected. Each node $v \in \mathcal{V}$ can be associated with node attributes as $X_v \in \mathbb{R}^{d_v}$. Similarly, each edge $e_{ij} : (v_i, v_j) \in \mathcal{E}$ can also have attributes noted as $E_{ij} \in \mathbb{R}^{d_e}$. Here, d_v and d_e are dimension of node features and edge features, respectively.

Table 1: Operands/Variables in specification ϕ and system B .

Operands/ Variables	Specification ϕ				System B		
	\mathcal{A}	$\tilde{\mathcal{A}}$	true(1)	false(N)	\mathcal{A}	$\neg\mathcal{A}$	true(1)
Meaning	a to z	$!a$ to $!z$	$a \mid !a, a \in \mathcal{A}$	$a \ \& \ !a, a \in \mathcal{A}$	a to z	$\neg a$ to $\neg z$	$a \mid \neg a, a \in \mathcal{A}$
Cardinality	26	26	1	1	26	26	1

GNNs aim to learn a vector representation \mathbf{h}_v for each node v by aggregating the neighbourhood information and iteratively updating its own hidden representation through k hops as

$$\mathbf{h}_v^k = \text{UPDATE}(\mathbf{h}_v^{k-1}, \text{AGGREGATE}(\{\mathbf{h}_u^{k-1} \mid u \in \mathcal{N}_v\})).$$

Here, UPDATE is implemented by neural networks while AGGREGATE is a pooling operation that is invariant to the permutation of the neighbors \mathcal{N}_v regarding node v . GNNs combine structural information and node features via message passing on the given graph \mathcal{G} . In contrast to standard neural networks, it has the capacity to retain the node representation captured by propagation up to any depth. Recently, GNNs have achieved groundbreaking success on tasks with graph-structured data, especially in node classification [30, 25, 40] and graph classification [28, 16]. This motivates us to exploit the structural property of B and ϕ , and then represent them as graphs for classification, where the goal is to determine whether B satisfies ϕ or not.

3 OCTAL: LTL Model Checking via Graph Representation Learningsec:Method

OCTAL determines whether a system, represented by a Büchi automaton B satisfies a specification ϕ represented by an LTL formula through their unified graph representations. We formulate the problem as supervised learning on graphs, where the input B and ϕ along with the corresponding label ('0/1') are provided during training, where '1' indicates that B satisfies ϕ and '0' otherwise.

3.1 Variables and Operators

The systems and specifications we deal with are constructed from the operands/variables \mathcal{A} , operators $\mathcal{O} = \{G, F, R, W, M, X, U, !, \&, \mid\}$ and special variables **true(1)** and **false(N)**, the specifics of which are described in Table 1 above and Table 6 in Appendix A. Each variable and operator has a distinct meaning and share across B and ϕ . A variable has its true or negated form (noted as $\tilde{\mathcal{A}}$ or $\neg\mathcal{A}$).

3.2 Representation of System and Specification

System Graph \mathcal{G} We represent B as a bipartite graph $\mathcal{G} = (V_{\mathcal{G}}, E_{\mathcal{G}})$, where $V_{\mathcal{G}} = V_s \cup V_e$ and $E_{\mathcal{G}} \subseteq V_s \times V_e$. Here, V_s of nodes are the states of B , and V_e of nodes are the transitions of B . There is an edge between $v_i \in V_s$ and $v_j \in V_e$ if and only if v_i is the source or destination state of the transition v_j in B . \mathcal{G} is undirected in nature, but it can be extended to a directed version.

Figures 2(a) and 2(b) illustrate B and the corresponding bipartite graph \mathcal{G} . The two states q_0 and q_f form the set V_s , and the transitions E_1, E_2 and E_3 form the set V_e . Since q_0 is a source and destination state for E_1 , and a source state for E_3 , there is an edge between q_0 and E_1 , and q_0 and E_3 respectively. This is analogously followed by the rest of the graph. The intuition behind representing B as a bipartite graph is to capture the transition labels. Since we aim to learn the overall representation of a given system, both states and transitions in B play an essential role here. A state transits into another state if and only if the transition label is satisfied. To learn the semantic meaning through transitions and their corresponding labels, we map transitions as nodes as shown in Figure 2(b) accordingly, and therefore can obtain the representation for them, which is a function of the labels pertaining to the transition.

Specification Graph \mathcal{T} Every LTL formula can be represented as an expression tree $\mathcal{T} = (V_{\mathcal{T}}, E_{\mathcal{T}})$ (see Figure 2(c)), which is constructed based on the precedence and associativity of the operators in LTL formulae, described as follows: 1) ϕ is converted to its postfix form, which is used to construct the expression tree; 2) The operators exhibit right associativity, where the unary operators $\{!, G, F, X\}$ have the highest priority. 3) The binary temporal operators $\{U, R, W, M\}$ have the second highest priority, and the boolean connectives $\{\&, \mid\}$ have the lowest priority.

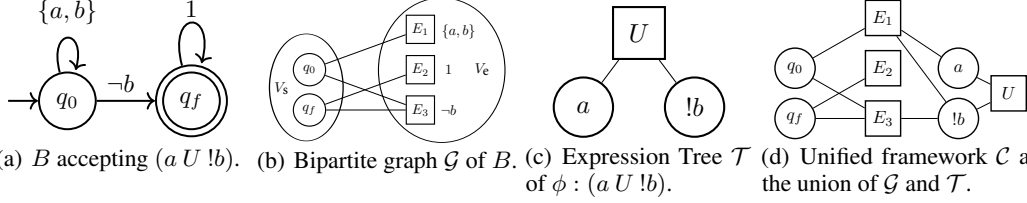


Figure 2: Illustration of system B , bipartite graph \mathcal{G} , expression tree \mathcal{T} for specification ϕ , and the unified framework \mathcal{C} approximating $B' = B \times B_{\neg\phi}$, but with polynomial complexity of $|B + \phi|$.

$V_{\mathcal{T}}$ constitutes the operators and operands of ϕ , and $E_{\mathcal{T}} \subseteq V_{\mathcal{T}} \times V_{\mathcal{T}}$. ϕ is represented in Negation Normal Form (NNF) [15], which would place $!$ only before the operands. This allows us to represent $!a$ as a variable in $\tilde{\mathcal{A}}$ and eliminate the $!$ operator. For example, the NNF equivalent of $!(a U b)$ is $!a R !b$. Here, the $!$ operator is present only before a and b in the NNF equivalent of the formula $!(a U b)$. Another compelling reason for representing ϕ in NNF is that transitions of B comprise of labels in $\text{true}(1)$, \mathcal{A} , and $\neg\mathcal{A}$. Representing negation *only* before variables and eliminating the $!$ operator from ϕ enables the shared representation for variables across B and ϕ . As a result, there is no semantic difference between $\neg\mathcal{A}$ and $\tilde{\mathcal{A}}$: $\neg a \in \neg\mathcal{A}$ may occur in a transition label of B and $!a \in \tilde{\mathcal{A}}$ may occur in a leaf node of ϕ , but both $\neg a$ and $!a$ signify that a does not hold.

3.3 Bridging System and Specification via Graph Union

To establish the relation between graphs of system \mathcal{G} and specification \mathcal{T} , we propose to construct the unified graph \mathcal{C} to model them jointly. As Figure 1 shows, traditional approaches of model checking computes the intersection of B and $B_{\neg\phi}$ by their cross product, which results in an automaton B' whose states are the product of the states of B and $B_{\neg\phi}$, and its transitions depend on the transition labels of both B and $B_{\neg\phi}$. Since our main goal is to avoid constructing $B_{\neg\phi}$ and thus B' , we directly feed the input graph without products to OCTAL and aim to use neural networks to learn the latent correspondence by combining \mathcal{G} and \mathcal{T} as a joint framework \mathcal{C} in the following way. Each transition label consists of operands and variables in \mathcal{A} or $\neg\mathcal{A}$, which is shared across the system and specification. Based on this observation, we join graphs \mathcal{G} and \mathcal{T} by adding a link between the corresponding nodes $V_e \in \mathcal{G}$ and $V_{\mathcal{T}} \in \mathcal{T}$ if they contain the same variable/operand that belongs to \mathcal{A} or $\tilde{\mathcal{A}}/\neg\mathcal{A}$. Figure 2(d) shows the result of such graph union between \mathcal{G} and \mathcal{T} . Here, there is an edge between a and E_1 as a is contained in E_1 . Similarly, there is one edge between $!b$ and E_1 , and the other between $!b$ and E_3 as b is in E_1 and $\neg b$ is in E_3 .

Formally, the unified framework is a joint graph $\mathcal{C} = (V_{\mathcal{C}}, E_{\mathcal{C}})$ represented as the union of \mathcal{G} and \mathcal{T} , where $V_{\mathcal{C}} = V_{\mathcal{G}} \cup V_{\mathcal{T}}$, and $E_{\mathcal{C}} \subseteq V_{\mathcal{C}} \times V_{\mathcal{C}}$ such that, there is an edge between every leaf node $l \in V_{\mathcal{T}}$, and nodes $E \in V_e$ such that l contains a variable $a \in \mathcal{A}$ or $!a \in \tilde{\mathcal{A}}$, and E also contains the same/equivalent variable $a \in \mathcal{A}$ or $\neg a \in \neg\mathcal{A}$.

3.4 Node Encoding

Each node $v \in \mathcal{C}$ consisting of operands/variables is represented by a vector as follows

$$\left\{ \underbrace{[_]}_{1/0} \underbrace{[_, _, _, \dots, _]}_{\forall a \in \mathcal{A}} \underbrace{[_, _, _, \dots, _]}_{!a/\neg a, \forall a \in \mathcal{A}} \underbrace{[_, _, _, \dots, _]}_{\forall o \in \{\mathcal{O}/!\}} \underbrace{[_, _]}_{q \in Q} \right\}$$

Part I of 1 bit is reserved for the special variable **true**(1) or **false**(N). Part II encodes $\forall a \in \mathcal{A}$, with size of $|\mathcal{A}|$. Part III of size $|\mathcal{A}|$ encodes variables/operands in either $\neg\mathcal{A}$ or $\tilde{\mathcal{A}}$, as both of them are semantically equivalent. Part IV corresponds to operators in \mathcal{O} except $!$, with the size of $|\mathcal{O}| - 1$. The last part V represents the type of state q of B in 2 bits. Part I and V use one-hot encoding for indication. Each variable/operand has a distinct meaning but sharing across \mathcal{G} and \mathcal{T} . Without loss of generality, the value of $i \in \mathcal{A} \cup \mathcal{O}$ is sampled from a normal distribution $\mathcal{N}(\mu_i, \sigma)$ with a distinct mean μ_i and the controlled variance σ to avoid overlaps. The true form a and negated form $!a/\neg a$ of a variable share the same value but are located in different sections (\mathcal{A} in Part II, $\neg\mathcal{A}/\tilde{\mathcal{A}}$ in Part III).

Table 2: Summary statistics of datasets.

Dataset	Len_LTL	#State	#Transition	#Sample
Short	[1 - 80]	[1 - 95]	[1 - 1,711]	9,424
Diverse	[1 - 144]	[1 - 2,234]	[1 - 397,814]	6,107
RERS19	[3 - 39]	[1 - 21]	[3 - 157]	1,798

3.5 Learning Unified Graph for Modeling Checking

GNNs as a powerful tool can capture both structural information and node features for graph-structured data through propagation and aggregation of information in local neighborhoods. The message passing framework of GNNs is ideal for exploiting the structural correspondence between the automaton and LTL formula as well as the semantic meaning of transitions. Graph Isomorphism Network (GIN, [28]), one of the most expressive GRL models, is employed to learn the representation of the unified framework \mathcal{C} . GIN has demonstrated great performance in graph classification tasks and is expected to obtain better representation of graphs with complex structures. The key intuition here is to jointly learn the representation \mathcal{G} and \mathcal{T} . Since two structurally similar B 's (or ϕ 's) can represent different behaviors depending on the contents of the transition, both structure and labels that describe the semantics of the system (or specification) are equally important for LTL model checking. Modeling the system or the specification separately would lose such crucial connection between them, which is also the essential component in traditional model checkers formed as graph products. Hence, we deploy GIN to capture both structure and semantics of B and ϕ jointly in the representation learnt, and the significance of the joint representation for \mathcal{C} is further solidified in Sections 4.3 and 4.5.

4 Evaluation

4.1 Dataset

We present three datasets for LTL model checking: `Short` and `Diverse` are created through Spot [17], while `RERS19` is obtained from the annual competition RERS19 [27]. The data generated from Spot and provided by RERS19 are specifications, i.e., a set of LTL formulae ϕ 's. To generate the corresponding automaton B for each ϕ , the tool LTL3BA [3] is used, due to its superior speed [8]. Dataset `Short` consists of short-size specifications, all of which can be solved by LTL3BA within the time limit (2 mins). `Short` aims to test the checking speed of models w.r.t LTL3BA. Dataset `Diverse` comprises of complex and lengthy specifications, which LTL3BA times out for certain instances. `Diverse` is designed to test model's generalization ability for varied length of specifications, along with the speedup. `RERS19` is a standard benchmark for sequential LTL from the RERS19 competition. The statistics of datasets are summarized in Table 2, and detailed in Appendix B.2.

4.2 Experimental Settings

Training OCTAL is trained on `Short` and `Diverse` datasets with an 80-20 split between training and validation sets, which contain *equal* number of positive and negative samples for classification, and are randomly shuffled before splitting. We use Adam [29] to optimize model parameters with the initial learning rate $1e-5$, dropout value of 0.1, and the Binary Classification Entropy as the loss function for all our experiments. Early stopping is adopted when the highest accuracy on validation no longer increases for five consecutive checkpoints. All experiments are run 5 times independently, and the average performance and standard deviations are reported. Additional experiments and analysis including generalization of different models on `Diverse`, one-hot node encoding scheme and the directed version of \mathcal{G} are presented in Appendix C.

Evaluation Metrics Two settings are designed to evaluate the model: binary classification and one-vs-many. Accuracy, Precision and Recall are used for binary classification of pair-wise LTL-BA. The ranking metrics Hits@K and Mean Reciprocal Rank (MRR) are adopted for one-vs-many case. Hit@K counts the ratio of positive samples ranked at the top-K place against all the negative ones. MRR firstly calculates the inverse of the ranking of the first correct prediction against the given negative samples (50 by default), and then an average is taken over the total candidates.

Baselines Two class of methods are selected to compare for LTL model checking:

Table 3: Classification accuracy and precision/recall for LTL model checking. RERS19(S) and RERS19(D) represent LTL-BA being trained on Short and Diverse, and then tested on RERS19.

Models		Short	Diverse	RERS19(S)	RERS19(D)
Accuracy	MLP	65.42±1.75	58.13±1.13	64.80±4.28	48.96±2.37
	LinkPredictor	89.57±0.76	73.73±1.53	84.60±1.17	75.00±2.32
	OCTAL(GCN)	96.02±0.45	85.91±1.04	91.58±0.63	87.02±4.10
	OCTAL(GIN)	96.62±0.31	86.74±0.84	94.09±1.34	94.20±0.88
OCTAL	Precision	96.43±1.33	84.50±1.15	98.07±0.48	91.35±1.04
	Recall	96.86±0.97	88.70±0.91	89.97±3.00	97.64±1.19

Table 4: Running time (inference) of different models for LTL model checking.

Dataset	LTL3BA	MLP	LinkPredictor	OCTAL	Overhead
Short	91s	0.28s	0.39s	0.38s	33s
Diverse	43m	0.43s	0.74s	0.55s	9m
RERS19	17s	0.29s	0.22s	0.27s	6.3s

Traditional Model Checkers LTL3BA, LTL2BA [21], Spin [26] and Spot are the SOTA tools that perform the traditional way of symbolic model checking. These tools perform a set of optimizations on top of traditional model checking algorithms, and are capable of solving complex systems and specifications of varying lengths. LTL3BA is the fastest tool among them in terms of generating B corresponding to ϕ and checking for their equivalence. Therefore, we select LTL3BA as the strongest baseline for speed test: run it with a timeout of 2 minutes per LTL-BA pair, and the pairs it fails to model check within the time constraint are marked with the output ‘unknown’ and recorded the run-time as the upper limit.

Learning-based Models All neural networks take the unified framework \mathcal{C} as input, and outputs ‘0/1’: **MLP** A multilayer perceptron (MLP, [20]) classifier directly uses the given raw node features as input without utilizing graph structure of the unified framework \mathcal{C} for model checking.

LinkPredictor Graph Convolutional Network (GCN, [30]) is used to learn representations of \mathcal{G} and \mathcal{T} *separately*. The obtained graph embeddings of \mathcal{G} and \mathcal{T} are multiplied/concatenated and then fed into linear layers for classification, which essentially converts the satisfiability checking problem between \mathcal{G} and \mathcal{T} to a link prediction task.

OCTAL A GRL framework that reduces the model checking to a graph classification task by *jointly* learning the representation of \mathcal{G} and \mathcal{T} through the unified framework \mathcal{C} . The resultant node embeddings are aggregated using mean pooling to obtain the embedding for the unified graph, which is later fed into an MLP classifier for prediction. There are two variants: the default one uses 3-layer GIN noted as OCTAL (GIN), the other adopts 3-layer GCN as OCTAL (GCN).

4.3 Performance Analysis

Table 3 (upper) shows the performance of different methods for LTL model checking as a classification task. OCTAL (GIN) consistently outperforms all the other baselines, and achieves above 90% accuracy on three of four scenarios. OCTAL (GCN) also obtains above 85% accuracy, but on average slightly behind OCTAL (GIN), due to GCN’s limited expressiveness compared to GIN. In general, message passing frameworks of OCTAL perform much better than MLP and LinkPredictor, which either do not take graph structures into account or model systems and specifications separately. This validates the importance of OCTAL that jointly learning the representation of both system and specification, and their semantic correspondence under the unified framework via message passing.

To better evaluate the generalization capability of models, the domain shift learning between datasets is considered: Short \rightarrow RERS19 as RERS19(S) and Diverse \rightarrow RERS19 as RERS19(D). Comparing the left and right side results in Table 3, there is certain performance decay (5% \sim 10% drops) from MLP and LinkPredictor, which demonstrates their poor generalization when the domain shifts, and thus indicates their limited practical value. OCTAL generally maintains or even exceeds performance after domain shifting, and significantly outperform other two baselines (over 7% gap). This implies great stability and generalization of OCTAL between datasets with different patterns of systems and varying-length of LTL formulae, which is one of key metrics for real applications in production line.

Table 5: LEFT: One-vs-many results of different models for LTL model checking. RIGHT: Classification accuracy on *Short* with structural perturbation (Edges are dropped under certain probability).

Models	RERS19(S)		RERS19(D)		Short with Structural Perturbation		
	MRR	Hits@3	MRR	Hits@3	30%	50%	100%
MLP	24.15	25.58	12.02	10.17	50.00±0.00	50.00±0.00	50.00±0.00
LinkPredictor	55.77	73.08	31.77	35.50	50.00±0.00	50.00±0.00	50.00±0.00
OCTAL (GCN)	73.41	88.64	65.14	80.47	61.75±0.20	61.75±3.20	51.93±0.40
OCTAL (GIN)	95.74	97.78	77.17	88.21	83.59±1.60	79.44±0.23	50.52±0.39

To further validate the effectiveness of OCTAL for practical use, we present the metrics precision and recall in Table 3 (down). OCTAL consistently achieves around 90% precision and recall across all datasets. As the result suggests, OCTAL has a low false positive rate, and can accurately retrieve over 88% true positive samples from all three test sets, thus illustrating its usefulness in real applications, such as software verification (case study in Section 4.5).

4.4 Runtime and Complexity Analysis

Table 4 shows the runtime of both the tradition and learning-based model checkers for satisfiability checking of all samples in the listed dataset. For fair comparison, we include the graph preprocessing time as the overhead for neural network (NN) models since they take the unified framework \mathcal{C} as input, where constructing graphs \mathcal{G} and \mathcal{T} is required in prior. NN-based models show similar runtime as all of them take less than 1s for inference. Compared to traditional model checkers, with preprocessing overhead considered, NN-based models are still much faster than LTL3BA under every scenario. OCTAL as the most accurate NN models, achieves speedups of $\sim 3\times$, $\sim 5\times$ and $\sim 3\times$ over LTL3BA, on *Short*, *Diverse* and *RERS19*, respectively. It is worth noting that, in terms of inference time alone, OCTAL is $\sim 239\times$, $\sim 4690\times$, and $\sim 63\times$ faster than LTL3BA on these three datasets, respectively. This leads us to conclude that OCTAL can outperform the SOTA traditional model checkers with respect to speed, along with consistent accuracy across different datasets. Note that, as a proof of concept, the graph preprocessing time presented above is not extensively optimized in terms of speed. We aim to provide a parallel graph construction algorithm later that would significantly reduce the preprocessing overhead.

Traditional model checkers need map $\neg\phi$ to $B_{\neg\phi}$, compute the product $B' = B_{\neg\phi} \times B$, and then check emptiness of B' . The use of the union operation pairing with GRL framework enables OCTAL to avoid such non-polynomial complexity of graph products. Accordingly, the complexity of our proposed method is reduced to polynomial in the size of $|B + \phi|$. In the Sequential LTL Track of RERS19 competition, the top three teams managed to solve 100%, 65% and 25% of the given problems, respectively. The results presented did not include time, hence we are unable to make a comparison with respect to runtime for OCTAL against the leaderboard. However, we can still conclude that OCTAL beats the 2nd and 3rd teams by a large margin in terms of the number of problems it correctly solved (>90%) combining with its superior runtime and efficiency.

4.5 Case Study: Ranking and Robustness in Software Verification

Table 5 LEFT shows the results for LTL model checking on one-vs-many case. The test set RERS19 is constructed such that for every B , there is only one ϕ where B does satisfy and fifty other ϕ 's do not. Hence, every system is paired with one positive and fifty negative specifications. The goal of this task is to examine whether a model could distinguish the positive sample out of many changing negative ones, which is imitating real scenarios in software verification, by which OCTAL is strongly motivated. The metric Hit@3 is used to count the percentage of positive samples ranked top-3 against all the negative ones. We observe a large margin (consistently over 15%) between two NN-based models and two OCTAL variants, especially on RERS19(D). Furthermore, OCTAL outperforms LinkPredictor and MLP on all metrics. This again demonstrates the inherent limitation of graph-agnostic models that fail to capture the semantic correspondence between the system and the specification. The analysis also leads us to observe the generalization power of OCTAL, as it can identify a positive sample with very high confidence among a bunch of negative samples, thus making it feasible to be deployed in real world applications of software development.

Table 5 RIGHT shows the results when a percentage of edges is randomly dropped from the input graph. This case evaluates the robustness of OCTAL as well as the significance of the unified framework \mathcal{C} . The positive and negative pairs of Short are generated as follows: if B_r satisfies ϕ_r , then $\langle B_r, \phi_r \rangle$ is a positive pair. Let $p\%$ of transitions (edges) in \mathcal{G} be dropped from B_r , and the modified automaton be B'_r . B'_r does not accept ϕ_r as all constructed automata do not contain redundant transitions. Thus, dropping even one transition would lead $\langle B'_r, \phi_r \rangle$ to be a negative pair. When $p = 100\%$ corresponds to the case that all the edges in \mathcal{G} are dropped, then transition nodes V_e and state nodes V_s are completely isolated. Results from Table 5 clearly depict the importance of graph structure as MLP and LinkPredictor fail to generalize with perturbed input and give random guess under this setting. Since they completely overlook or only partially consider the structure and connection within the graph input, MLP and LinkPredictor cannot tell the difference between positive and negative samples: the input are identical for graph-agnostic models with or without edges. Therefore, just relying on node features is not a feasible solution when edges are dropped or \mathcal{G} is corrupted this way. On the other hand, message passing frameworks perform better as OCTAL (GIN) still holds the distinguishing ability for perturbation and achieves good generalization when the dropping range is between 30% and 50%. When $p = 100\%$, every transition in B is dropped, thus also leading to poor performance, that validates the importance of structural information for model checking. When $p < 30\%$, B_r and B'_r have large portion structural overlaps, leading to similar latent representations learnt by GNN models. This setting is very challenging and uncommon in practice, as different software implementations would lead to more than moderate structure changes in the system. Nevertheless, OCTAL can be further enhanced by adding regularization terms or via adversarial training to obtain high-level sensitivity for such special needs, which we leave for future study.

5 Related Work

To the best of our knowledge, this is the first work that applies graph representation learning to solve LTL-based model checking. Previously, the most relevant work to us was using GNNs to solve SAT for boolean satisfiability [37], satisfiability of 2QBF formulae [41], and automated proof search [33] in the higher order logic space. Regarding model checking, learning-based approaches have been used to select the most suitable model checker for an appropriate property and program [38]. Borges et al. [9] attempts to learn how to reshape a system expressed by NuSMV [11] to satisfy the property in temporal logic. Hahn et al. [24] trains a transformer to predict a satisfiable trace for an LTL formula. Zhu et al. [43] proposes model checking based on binary classification of machine learning. They represent the system using Kripke structures and specification using LTL formulae, and then served as input features to supervised learning algorithms, such as Random Forest, Decision Trees, Boosted Tree and Logistic Regression, which achieve similar accuracy as classical LTL model checking counterparts while partially avoiding the state space explosion problem. However, these ML-based algorithms do not generalize well when tested with formulae of varying lengths. Behjati et al. [5] proposes a reinforcement learning based approach for on-the-fly LTL model checking, which is designed to look for invalid runs or counterexamples by awarding heuristics with a agent. Their approach performs much faster than the classical model checkers and can verify systems with large state spaces, but the state space that an agent can reach is still bounded.

6 Conclusions and Future Work

OCTAL is a novel graph representation learning based framework for LTL model checking. It can be extremely useful for the first line of software development cycle, as it offers reasonable accuracy and robustness for early and quick verification of model checking compared to time-consuming unit tests and other efforts in ensuring the correctness of a given system. OCTAL is not intended to replace traditional model checkers, rather it makes model checking affordable and scalable for scenarios where traditional model checkers are infeasible. It would broaden the scope and use of model checking on a variety of less safety critical systems, by providing low-cost inference with high accuracy and robustness. It can also be enhanced with guarantee provided by applying traditional model checkers to limited candidates filtered by OCTAL.

In future, we would like to extend OCTAL to study its generalization for semantically equivalent formulae that may or may not vary in size and variables. In addition, it is very promising for OCTAL to support the generation of a counter example trace for the ‘no’ answers. Since the counter example generation is a relatively easier problem, tentatively, the user can invoke a traditional model checker to obtain it. In fact, they would only pay a low cost by deploying OCTAL as the ratio of false negatives

for the domain shifting task RERS19(S) and RERS19(D) is less than 10% and 3%, respectively. Meanwhile, recent developments such as GNNExplainer [42] and Gem [32] can be incorporated to identify the graph structures (node/edge/subgraph) that trigger OCTAL to conclude that B does not satisfy ϕ , which brings better interpretation of OCTAL. We believe this would further solidify OCTAL's claims and reduce dependency on traditional model checkers.

References

- [1] Abien Fred Agarap. 2018. Deep learning using rectified linear units (relu). *arXiv preprint arXiv:1803.08375* (2018).
- [2] Alessandro Armando, Roberto Carbone, and Luca Compagna. 2009. LTL model checking for security protocols. *Journal of Applied Non-Classical Logics* 19, 4 (2009), 403–429.
- [3] Tomáš Babiak, Mojmír Kretínský, Vojtech Reháč, and Jan Strejček. 2012. LTL to Büchi Automata Translation: Fast and More Deterministic. In *Proceedings of the 18th International Conference of Tools and Algorithms for the Construction and Analysis of Systems*, Vol. 7214. Springer, 95–109.
- [4] Jiri Barnat, Petr Bauch, Lubos Brim, and Milan Ceska. 2012. Designing fast LTL model checking algorithms for many-core GPUs. *J. Parallel Distributed Comput.* 72, 9 (2012), 1083–1097.
- [5] Razieh Behjati, Marjan Sirjani, and Majid Nili Ahmadabadi. 2010. Bounded Rational Search for On-the-Fly Model Checking of LTL Properties. In *Fundamentals of Software Engineering*. Springer Berlin Heidelberg.
- [6] Mordechai Ben-Ari, Amir Pnueli, and Zohar Manna. 1983. The Temporal Logic of Branching Time. *Acta Informatica* 20 (1983), 207–226.
- [7] Armin Biere, Alessandro Cimatti, Edmund Clarke, and Yunshan Zhu. 1999. Symbolic model checking without BDDs. In *International conference on tools and algorithms for the construction and analysis of systems*. Springer, 193–207.
- [8] František Blahoudek, Alexandre Duret-Lutz, Mojmír Křetínský, and Jan Strejček. 2014. Is There a Best Büchi Automaton for Explicit Model Checking?. In *Proceedings of the 2014 International SPIN Symposium on Model Checking of Software*. 68–76.
- [9] Rafael V. Borges, Artur S. d’Avila Garcez, and Luís C. Lamb. 2010. Integrating model verification and self-adaptation. In *Proceedings of the 25th International Conference on Automated Software Engineering*.
- [10] J. Richard Büchi. 1990. *On a Decision Method in Restricted Second Order Arithmetic*. Springer New York, 425–435.
- [11] Alessandro Cimatti, Edmund Clarke, Fausto Giunchiglia, and Marco Roveri. 1999. NuSMV: A new symbolic model verifier. In *Proceedings of the 11th International Conference on Computer Aided Verification*. Springer, 495–499.
- [12] E.M. Clarke, O. Grumberg, D. Kroening, D. Peled, and H. Veith. 2018. *Model Checking, second edition*. MIT Press.
- [13] Edmund M. Clarke, E. Allen Emerson, Somesh Jha, and A. Prasad Sistla. 1998. Symmetry Reductions in Model Checking. In *Proceedings of the 10th International Conference of Computer Aided Verification*, Vol. 1427. Springer, 147–158.
- [14] Edmund M. Clarke, Somesh Jha, Reinhard Enders, and Thomas Filkorn. 1996. Exploiting Symmetry in Temporal Logic Model Checking. *Formal Methods Syst. Des.* 9, 1/2 (1996), 77–104.
- [15] Adnan Darwiche. 2001. Decomposable negation normal form. *Journal of the ACM (JACM)* 48, 4 (2001), 608–647.

- [16] Manh Tuan Do, Noseong Park, and Kijung Shin. 2020. Two-stage Training of Graph Neural Networks for Graph Classification. *arXiv preprint arXiv:2011.05097* (2020).
- [17] Alexandre Duret-Lutz, Alexandre Lewkowicz, Amaury Fauchille, Thibaud Michaud, Etienne Renault, and Laurent Xu. 2016. Spot 2.0 — a framework for LTL and ω -automata manipulation. In *Proceedings of the 14th International Symposium on Automated Technology for Verification and Analysis*, Vol. 9938. Springer, 122–129.
- [18] E. Allen Emerson and Edmund M. Clarke. 1982. Using Branching Time Temporal Logic to Synthesize Synchronization Skeletons. *Sci. Comput. Program.* 2, 3 (1982), 241–266.
- [19] Matthias Fey and Jan Eric Lenssen. 2019. Fast graph representation learning with PyTorch Geometric. *arXiv preprint arXiv:1903.02428* (2019).
- [20] M.W Gardner and S.R Dorling. 1998. Artificial neural networks (the multilayer perceptron)—a review of applications in the atmospheric sciences. *Atmospheric Environment* 32, 14 (1998), 2627–2636.
- [21] Paul Gastin and D Oddoux. 2001. LTL 2 BA: fast translation from LTL formulae to Büchi automata.
- [22] Patrice Godefroid. 1991. Using Partial Orders to Improve Automatic Verification Methods. In *Proceedings of the 2nd International Workshop on Computer Aided Verification*. 176–185.
- [23] Viktor Gyuris and A. Prasad Sistla. 1997. On-the-Fly Model Checking Under Fairness That Exploits Symmetry. In *Proceedings of the 9th International Conference of Computer Aided Verification*, Vol. 1254. Springer, 232–243.
- [24] Christopher Hahn, Frederik Schmitt, Jens U. Kreber, Markus Norman Rabe, and Bernd Finkbeiner. 2021. Teaching Temporal Logics to Neural Networks. In *International Conference on Learning Representations*.
- [25] William L Hamilton, Rex Ying, and Jure Leskovec. 2017. Inductive representation learning on large graphs. In *Proceedings of the 31st International Conference on Neural Information Processing Systems*. 1025–1035.
- [26] Gerard J. Holzmann. 1997. The model checker SPIN. *IEEE Transactions on software engineering* 23, 5 (1997), 279–295.
- [27] Marc Jasper, Malte Mues, Alnis Murtovi, Maximilian Schlüter, Falk Howar, Bernhard Steffen, Markus Schordan, Dennis Hendriks, Ramon Schiffelers, Harco Kuppens, et al. 2019. RERS 2019: combining synthesis with real-world models. In *International Conference on Tools and Algorithms for the Construction and Analysis of Systems*. Springer, 101–115.
- [28] Jure Leskovec Keyulu Xu, Weihua Hu and Stefanie Jegelka. 2018. How Powerful are Graph Neural Networks?. In *International Conference on Learning Representations*.
- [29] Diederik P. Kingma and Jimmy Ba. 2015. Adam: A Method for Stochastic Optimization. In *International Conference on Learning Representations*.
- [30] Thomas N Kipf and Max Welling. 2017. Semi-supervised classification with graph convolutional networks. In *International Conference on Learning Representations*.
- [31] Carlos Delgado Kloos and Werner Damm. 2012. *Practical Formal Methods for Hardware Design*. Springer Science & Business Media.
- [32] Wanyu Lin, Hao Lan, and Baochun Li. 2021. Generative causal explanations for graph neural networks. In *International Conference on Machine Learning*. 6666–6679.
- [33] Aditya Paliwal, Sarah M. Loos, Markus N. Rabe, Kshitij Bansal, and Christian Szegedy. 2020. Graph Representations for Higher-Order Logic and Theorem Proving. In *The Thirty-Fourth AAAI Conference on Artificial Intelligence*. AAAI Press, 2967–2974.
- [34] Carl Adam Petri. 1983. Some Personal Views of Net Theory. In *Applications and Theory of Petri Nets*. Springer, 1–13.

- [35] Amir Pnueli. 1977. The Temporal Logic of Programs. In *Proceedings of the 18th Annual Symposium on Foundations of Computer Science*. IEEE Computer Society, 46–57.
- [36] A Saul. 1963. Kripke. Semantical analysis of modal logic I: Normal modal propositional calculi. *Zeitschrift für mathematische Logik und Grundlagen der Mathematik* 9, 5-6 (1963), 67–96.
- [37] Daniel Selsam, Matthew Lamm, Benedikt Bünz, Percy Liang, Leonardo de Moura, and David L. Dill. 2019. Learning a SAT Solver from Single-Bit Supervision. arXiv:1802.03685 [cs.AI]
- [38] Varun Tulsian, Aditya Kanade, Rahul Kumar, Akash Lal, and Aditya V. Nori. 2014. MUX: algorithm selection for software model checkers. In *Proceedings of the 11th Working Conference on Mining Software Repositories*. ACM, 132–141.
- [39] Antti Valmari. 1992. A stubborn attack on state explosion. *Formal Methods in System Design* 1, 4 (1992), 297–322.
- [40] Petar Veličković, Guillem Cucurull, Arantxa Casanova, Adriana Romero, Pietro Lio, and Yoshua Bengio. 2018. Graph attention networks. In *International Conference on Learning Representations*.
- [41] Zhanfu Yang, Fei Wang, Ziliang Chen, Guannan Wei, and Tiark Rompf. 2019. Graph Neural Reasoning for 2-Quantified Boolean Formula Solvers. *Workshop on Learning and Reasoning with Graph-Structured Representations (co-located with ICML)* (2019).
- [42] Rex Ying, Dylan Bourgeois, Jiaxuan You, Marinka Zitnik, and Jure Leskovec. 2019. GN-NEExplainer: Generating Explanations for Graph Neural Networks. In *Proceedings of the 33rd International Conference on Neural Information Processing Systems*.
- [43] Weijun Zhu, Huanmei Wu, and Miaolei Deng. 2019. LTL Model Checking Based on Binary Classification of Machine Learning. *IEEE Access* 7 (2019), 135703–135719.

Table 6: Temporal Operators in Linear Temporal Logic

Symbol	G	F	R	W	M	X	U
Meaning	globally	finally	release	weak until	strong release	next	until

A Temporal Operator Notations

The meaning of temporal operators supported by ϕ is presented in Table 6.

B Experimental Settings

B.1 Environment

Experiments were performed on a cluster with four Intel 24-Core Gold 6248R CPUs, 1TB DRAM, and eight NVIDIA QUADRO RTX 6000 (24GB) GPUs.

B.2 Dataset Description

The specifications (ϕ) for `Short` and `Diverse` are constructed by `Spot`. The corresponding systems (B) for specifications of both `Spot` generated and `RERS` are created by `LTL3BA`.

These three datasets are constructed to test the generalization capability of `OCTAL` across different distributions and varying length specifications. The distribution of `Diverse` subsumes `Short` and `RERS19`, and comprises of the most complex and lengthy specifications and corresponding systems, for which `LTL3BA` takes the longest time. Dataset `Diverse` is designed to test the performance of `OCTAL` on diversified samples, where the ability of generalization is examined via varying length systems and specifications presented in the evaluation across different scenarios, where previous related works such as [43] are suffered from.

B.2.1 Spot Generated Datasets

The `randltl` feature of `Spot` controls the length of generated LTL formulae, where the default size of expression tree is set to 15. The output formulae are not syntactically the same and less than 10% of them are semantically equivalent. There are two types of datasets generated through `Spot`: `Short`, where the length of the LTL formulae (noted as `#Lens`) range from 1 to 80 and `Diverse`, where the length of the LTL formulae range from 1 to 144. The length distribution of the formula for both `Short` and `Diverse` is plotted in Figures 3(a) and 4(a). The number of states and edges of these two datasets are described in Figures 3(b), 3(c), 4(b), and 4(c), respectively. By observing those distributions, it can be concluded that `Diverse` comprises of the largest automata and an uniform length distribution of LTL formulae. The range of length and states of LTL formulae is similar between `Short` and `RERS19`, but the corresponding transition range is less than 160 for `RERS19` while 1,711 for `Short`. The distribution pattern of both ϕ and B for dataset `Diverse` is quite different from the other two datasets.

B.2.2 RERS Dataset

Rigorous Examination of Reactive Systems (RERS) is an international model checking competition track organized every year. We adopt 1800 problems from the Sequential LTL track and compare the performance of `OCTAL` with respect to the top 3 teams on the leaderboard, in terms of accuracy under time constraints. The statistical details of dataset `RERS19` is presented in Figure 5.

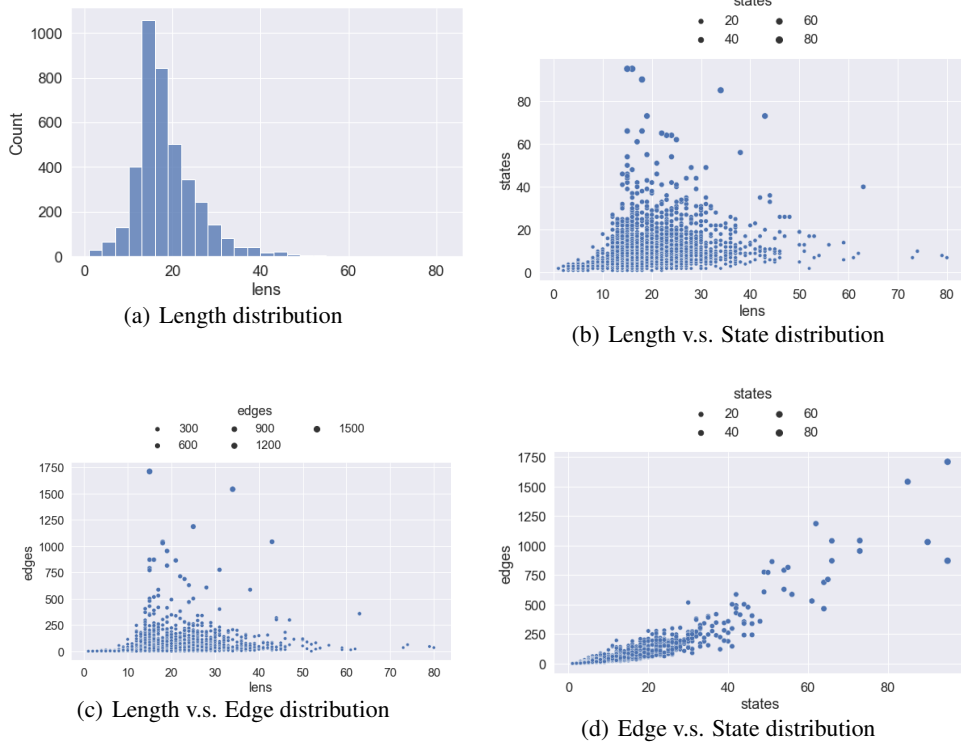


Figure 3: Statistical Summary of Dataset Short.

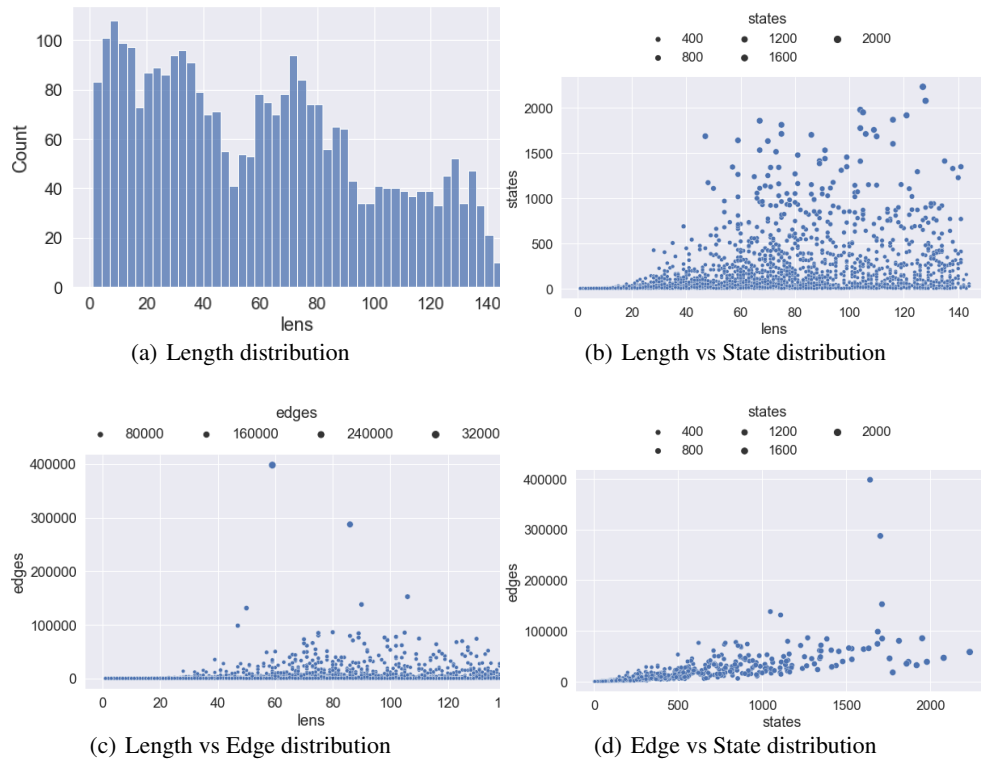


Figure 4: Statistical Summary of Dataset Diverse.

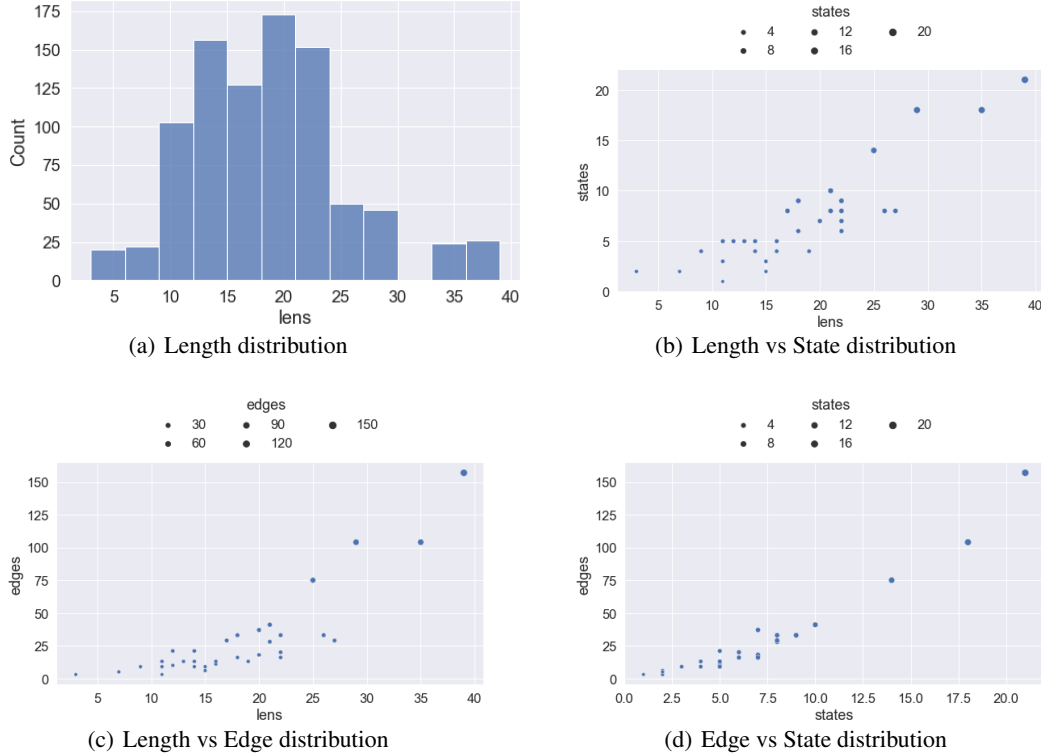


Figure 5: Statistical Summary of Dataset RERS19.

B.3 Architecture and Hyperparameters

The architecture of OCTAL (illustrated in Figure 6) comprises of a three-layer GNN, followed by a two-layer MLP to classify whether B satisfies ϕ . Mean pooling is used to aggregate the learnt node embeddings. A dropout rate of 0.1 is used, along with 1D batch normalization in every convolution layer of GNN. ReLU [1] is used as the non-linear activation between GNN and MLP layers. Every node in \mathcal{C} has an initial embedding of length 64 (or 66 for the directed \mathcal{G}). The GNN framework produces an embedding for \mathcal{C} of dimension 128 after mean pooling. MLPs take this hidden graph representation as the input, and produce a ‘0/1’ result as the final prediction.

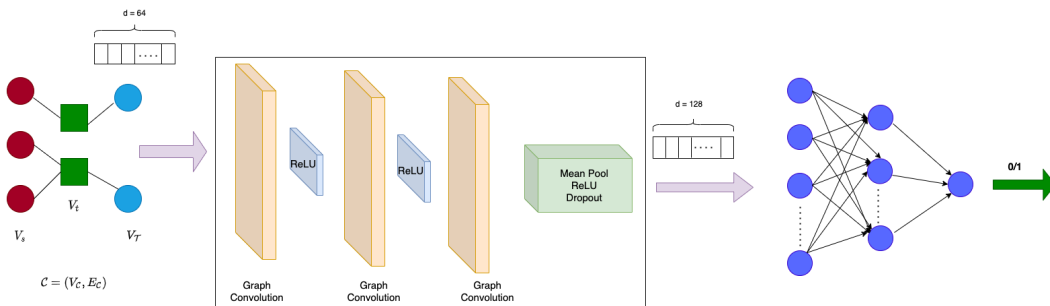


Figure 6: Overview of OCTAL Architecture.

B.4 Implementation Details

The code base is implemented on PyTorch 1.8.0 and pytorch-geometric [19]. The source files are attached along with the submitted supplementary.

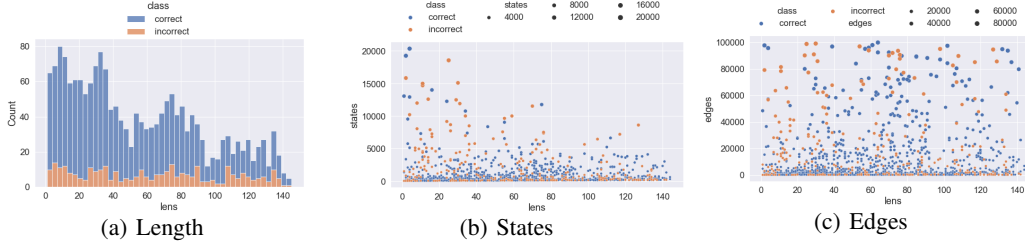


Figure 7: Distribution of Predicted Results on Dataset Diverse.

Table 7: Classification accuracy and precision/recall for one-hot encoding. RERS19(S) and RERS19(D) represent models being trained on Short and Diverse, and then tested on RERS19.

Models	Short	Diverse	RERS19(S)	RERS19(D)	
OCTAL	95.60±0.31	86.74±0.71	94.95±0.71	94.90±0.56	
OCTAL	Precision	95.47±0.39	86.26±1.54	97.02±0.59	92.55±0.90
	Recall	95.75±0.77	86.45±1.31	92.75±1.38	97.66±0.91

C Additional Experimental Results

C.1 Generalization on Dataset Diverse

We further tested the generalization of OCTAL on model checking problems with a larger and diverse distribution by training OCTAL on Short and testing with samples in Diverse. OCTAL (GIN) achieves 84.2% accuracy on average which is slightly decayed from the performance in Table 3 but still performs reasonably well across larger B 's and longer ϕ 's. Figure 7 shows the distribution of correctly and incorrectly predicted samples. OCTAL generalizes pretty well across varying length ϕ and for B 's of sizes much larger than the range of Short. The distribution pattern for the correct prediction is similar to Diverse's as shown in Figure 4, which indicates OCTAL can well generalize on unseen larger samples in testing.

C.2 Settings for One-hot Encoding

Instead of sampling from a normal distribution as described in Section 3.4, each variable/operator is represented with the value '1' in its respective position, if v contains the representation for it. Otherwise, the position has the value '0'. The rest rules for encoding remain the same.

C.3 Settings for \mathcal{G} irected

In addition to the node encoding presented in Section 3.4. Part VI is added and encodes the direction of state transitions for directed \mathcal{G} as following,

$$\left\{ \underbrace{\left[_ \right]}_{1/0} \underbrace{\left[_, _, _, \dots, _ \right]}_{\forall a \in \mathcal{A}} \underbrace{\left[_, _, _, \dots, _ \right]}_{!a / \neg a, \forall a \in \mathcal{A}} \underbrace{\left[_, _, _, \dots, _ \right]}_{\forall o \in \{\mathcal{O}/!\}} \underbrace{\left[_, _ \right]}_{q \in \mathcal{Q}} \underbrace{\left[_, _ \right]}_{v \in V_s} \right\}$$

In this case, the direction needs to be encoded only in \mathcal{G} , which is the bipartite representation of B . Every $v \in V_e$, stores the source and destination vertices of the corresponding transition. The first field represents the source $v_i \in V_s$, and the second field records the destination $v_j \in V_s$. Part VI of V_s and $V_{\mathcal{T}}$ would be all zeros as the direction of transitions is sufficiently encoded in V_e .

C.4 Analysis of Additional Results

The experimental results of one-hot encoding and Directed \mathcal{G} are presented in Tables 7 and 8, respectively. The experiments were run under similar settings for five independent runs, with mean and standard deviation reported for accuracy, precision and recall. Observed from those tables, OCTAL performs roughly well in general on all configurations of both one-hot and directed \mathcal{G} . For

Table 8: Classification accuracy and precision/recall for Directed \mathcal{G} . RERS19(S) and RERS19(D) represent models being trained on Short and Diverse, and then tested on RERS19.

Models	Short	Diverse	RERS19(S)	RERS19(D)	
OCTAL	95.75±0.77	87.55±0.40	95.17±1.50	94.48±0.51	
OCTAL	Precision	95.13±1.20	85.69±1.51	97.90±1.15	92.49±1.59
	Recall	97.20±0.55	89.06±2.50	92.37±4.08	96.88±1.89

one-hot encoding, it only slightly outperforms the original encoding on domain shift for RERS19 but could not obtain further gains on other two datasets as shown in Table 7. On comparison with the undirected \mathcal{G} presented in Table 3, OCTAL performs slightly better in general on Diverse with the directed \mathcal{G} . The rest of the configurations give comparable performance in terms of accuracy, precision and recall with respect to Table 8. From the results reported above, we can conclude that the current position specific representation for variables, their negated form, and operators are sufficient for OCTAL to obtain consistent performance, along with robust enough generalization capabilities and balanced computational cost.